

Comparison of Neuroplastic Responses to Cathodal Transcranial Direct Current Stimulation and Continuous Theta Burst Stimulation in Subacute Stroke

NICOLO, Pierre, *et al.*

Abstract

To investigate the effects of cathodal transcranial direct current stimulation (tDCS) and continuous theta burst stimulation (cTBS) on neural network connectivity and motor recovery in individuals with subacute stroke.

Reference

NICOLO, Pierre, *et al.* Comparison of Neuroplastic Responses to Cathodal Transcranial Direct Current Stimulation and Continuous Theta Burst Stimulation in Subacute Stroke. *Archives of Physical Medicine and Rehabilitation*, 2018, vol. 99, no. 5, p. 862-872.e1

DOI : 10.1016/j.apmr.2017.10.026

PMID : 29223708

Available at:

<http://archive-ouverte.unige.ch/unige:104793>

Disclaimer: layout of this document may differ from the published version.



UNIVERSITÉ
DE GENÈVE

Comparison of neuroplastic responses to cathodal transcranial direct current stimulation and continuous theta burst stimulation in subacute stroke

Abstract

Objective: To investigate the effects of cathodal transcranial direct current stimulation (tDCS) and continuous theta burst stimulation (cTBS) on neural network connectivity and motor recovery in individuals with subacute stroke.

Design: Double-blinded, randomized, placebo-controlled study.

Setting: Stroke subjects recruited through a university hospital rehabilitation program.

Participants: Stroke inpatients (N=41; mean age 65y, range 28-85; mean weeks poststroke 5, range 2-10) with resultant paresis in the upper extremity (mean Fugl-Meyer score 14, range 3-48).

Intervention: Stroke subjects were randomly assigned to neuronavigated cTBS (N=14), cathodal tDCS (N=14), or sham TMS/sham tDCS (N=13) over the contralesional primary motor area (M1). Each subject completed nine stimulation sessions over three weeks, combined with physical therapy.

Main outcome measures: Brain function was assessed with resting-state directed and non-directed functional connectivity based on high-density electroencephalography (EEG) before and after stimulation sessions. Primary clinical endpoint was the change in slope of multifaceted motor score composed of the Upper-Extremity Fugl-Meyer Assessment (UE-FMA), Box and Block test (BBT), Nine Hole Peg Test (NHPT), Jamar dynamometer between the baseline period and the treatment time.

Results; Neither stimulation treatment enhanced clinical motor gains. Cathodal tDCS and cTBS induced different neural effects. Only cTBS was able to reduce transcallosal influences from the contralesional to the ipsilesional M1 during rest. Conversely, tDCS enhanced perilesional beta-band oscillation coherence as compared to cTBS and sham groups. Correlation analyses indicated that the modulation of interhemispheric driving and perilesional beta-band connectivity were not independent mediators for functional recovery across all patients. However, exploratory subgroup analyses suggest that the enhancement of perilesional beta-band connectivity through tDCS might have more robust clinical gains if started within the first 4 weeks after stroke.

Conclusions: The inhibition of the contralesional primary motor cortex or the reduction of interhemispheric interactions was not clinically useful in heterogeneous group of subacute stroke subjects. An early modulation of perilesional oscillation coherence seems to be a more promising strategy for brain stimulation interventions.

Keywords: Cathodal transcranial direct current stimulation / Continuous theta-burst stimulation / Motor recovery / Stroke / Electroencephalography

42

43 **References:** 80

44 **Tables:** 3

45 **Figures:** 4

46

47 **Ethics approval:** Procedures were approved by the Local Ethics Committee.

48

49 **Abbreviations:** BBT: Box and Block Test; ca-tDCS: Cathodal tDCS; CMS: Compound
50 motor score; cTBS: Continuous theta burst stimulation; EEG: Electroencephalography;
51 FC: Functional connectivity; IPL: Inferior parietal lobule; M1; Primary motor cortex; MAL-
52 14: Motor Activity Log-14; MRI: Magnetic resonance imaging; NIBS: Non-invasive brain
53 stimulation; NHPT: Nine Hole Peg Test; NIHSS: National Institute Stroke Scale; PDC:
54 Partial directed coherence; rTMS: Repetitive transcranial magnetic stimulation; SMA:
55 Supplementary motor area; SnPM: Statistical non-parametric mapping; TBS: Theta burst
56 stimulation; tDCS: Transcranial direct current stimulation; UE-FMA: Upper-Extremity Fugl-
57 Meyer Assessment; WND: Weighted node degree.

Non-invasive brain stimulation (NIBS) has potential to boost training-dependent plasticity and promote motor recovery ¹⁻⁵. Repetitive transcranial magnetic stimulation (rTMS) and transcranial direct current stimulation (tDCS) are two frequently used neurostimulation methods that modulate cortical excitability. Despite their different mechanisms ^{1, 6}, they can both result in excitation or inhibition of neural activity at the stimulation site and in remote interconnected areas beyond the stimulus duration ⁷. In patients with unilateral stroke lesions, NIBS is thought to act on an imbalance in excitation and inhibition between hemispheres either by exciting ipsilesional motor areas or by inhibiting a hyperexcitability of contralesional motor nodes which is thought to exert a maladaptive inhibition on ipsilesional nodes ^{8, 9}.

The inhibitory strategy has the advantage of a reduced risk of seizure induction, in particular in patients with recent brain lesions ¹⁰⁻¹². Inhibitory rTMS or tDCS over contralesional motor nodes can reduce interhemispheric inhibition and increase excitability or connectivity of ipsilesional motor nodes ^{13, 14}. Some clinical trials using this approach have reported moderate motor gains ¹⁵⁻¹⁷, but studies in larger samples failed to replicate this benefit ¹⁸⁻²⁰.

One main reason for the disappointing effect sizes is that the response to brain stimulation is variable across subjects. Many patients even show a paradoxically reversed effect ²¹⁻²⁷. Furthermore, the model of interhemispheric inhibition has recently been questioned. It has been derived exclusively from patients with chronic stroke ²⁸⁻³⁰ and it remains unclear

80 if a rebalance between hemispheres is useful in subacute stages. Moreover, recent
81 studies have been unable to find clear evidence for a contralesional hyperexcitability in
82 large cohorts of subacute and chronic stroke subjects ³¹⁻³³, which raises questions on the
83 usefulness of an inhibition with NIBS. It is therefore important to monitor the neural effects
84 of NIBS and to test whether it can influence earlier and possibly more relevant functional
85 repair processes occurring during the first months after stroke.

86
87 From the animal literature, we know that cortical remapping and axonal sprouting are
88 accompanied by coherent neural oscillations between perilesional areas and surrounding
89 tissue ³⁴⁻³⁶. In human stroke subjects, we previously observed that the presence of
90 coherent alpha-band oscillations (as defined from electroencephalography, EEG) is
91 associated with better residual performance in motor tests ³⁶. For instance, the more the
92 ipsilesional primary motor cortex remained synchronized with the rest of the brain, the
93 better patients could move their upper limb ³⁶. We also identified pattern of network
94 interactions, which was predictive of future clinical improvement. The presence of
95 coherent spontaneous beta-band oscillations between the perilesional motor areas and
96 the rest of the brain was associated with greater clinical motor recovery observed in
97 subsequent months ³⁷. This synchronization has to occur within the first weeks after
98 stroke, as later increases of coherence were associated with worse recovery. Perilesional
99 oscillation coherence in alpha and beta frequencies is thus an interesting target for NIBS.

In this study, we therefore tested if NIBS could modulate interhemispheric interactions between the primary motor cortices, and/or the coherence of spontaneous perilesional neural activity and verified whether any of these modulations were able to boost clinical motor recovery in subjects with subacute stroke. In order to identify the stimulation technique which is most suitable for modulating the processes of interest, we compared two frequently used inhibitory NIBS techniques, continuous theta burst stimulation (cTBS) and cathodal tDCS (ca-tDCS) to sham stimulation, all applied to the contralesional primary motor cortex.

METHODS

Subjects

We screened one-hundred-eighty-four adult inpatients who were hospitalized at the Division of Neurorehabilitation of the University Hospital for hemispheric stroke from 2013 to 2016. Inclusion criteria were: (1) ischemic or hemorrhagic stroke; (2) ≤ 10 weeks after stroke; (3) unilateral lesion in the territory of the middle cerebral artery; and (4) first-ever appearance of upper extremity motor impairment based on Fugl-Meyer upper extremity scale (≤ 50). Participants were excluded if they met any of the following criteria: epileptic

121 seizures, presence of metallic objects in the brain, skull breach after craniectomy,
122 presence of implants or neural stimulators, pregnancy, sleep deprivation, recent traumatic
123 brain injury, delirium or disturbed vigilance, inability to participate in 1 h treatment sessions,
124 severe language comprehension deficits, new stroke lesions during rehabilitation, or
125 medical complications.

126
127 Forty-one subjects aged 28–85 years (mean 65 years; eighteen women; one left-handed;
128 twelve had left hemispheric stroke) were included in the study. On admission, the mean
129 National Institute Stroke Scale (NIHSS) was 12.8, range 2-24, mean Upper-Extremity
130 Fugl-Meyer Assessment (UE-FMA) was 13.8, range 3-48, mean delay between stroke
131 infarct and the first stimulation was 5.2 weeks, range 2-10. Patients' demographic and
132 clinical characteristics are compared between groups in Table 1. No significant differences
133 were observed for baseline parameters.

134
135 Sample size was determined with a power analysis which was based on the main
136 objective of our study: to test the clinical impact of NIBS on neural markers of plasticity.
137 From our previous studies ^{36, 37}, we can expect a correlation coefficient of about 0.7
138 between neural and clinical effects. A sample size of 14 per group gave us >80% power
139 to detect similar associations in this study.

140
141 All stroke subjects received an individually tailored multidisciplinary inpatient rehabilitation
142 program in the sub-acute phase, consisting of 60 minutes of physical therapy daily

(5x/week) with of active motor exercises of the upper-extremity. They gave written informed consent to all procedures. Procedures were approved by the Local Ethics Committee and conducted according to the Declaration of Helsinki. The trial was registered with ClinicalTrials.gov (number NCT02031107).

Study Design

This was a double-blinded, randomized, placebo-controlled, parallel-group study. Participants were randomly assigned to neuronavigated^c paired cTBS, ca-tDCS, or sham stimulation over the contralesional primary motor cortex. Subjects included in the sham group received either sham tDCS or sham cTBS in alternate order. Randomization was stratified for initial motor impairment and stroke lateralization, with an allocation sequence based on a block size of three, generated with a computer random-number generator by a researcher not involved in recruitment.

Motor function was assessed by a trained therapist who was blinded to treatment allocation: two pre-intervention baseline assessments separated by 1 week (T1 and T2), as well as post-intervention assessments after (T3) and 30-days after stimulation treatment (T4). Ten minutes of resting-state EEG were acquired at most 5 days prior to the first stimulation and 5 days after the last stimulation.

NIBS were applied in 3 sessions per week over 3 weeks. Subjects were blinded with respect to the true or sham stimulation conditions. NIBS were combined with 30 minutes of active functional motor practice. The therapy protocol contained a standardized set of exercises of varying difficulty and scope of which the therapist chose individually the ones which were most adapted for current impairment and objectives of each patient (see supplementary materials). In contrast, the researcher administering NIBS was unblinded. The overall study flow is shown in Figure 1.

Transcranial direct current stimulation (tDCS)

tDCS^a was applied for 25 minutes at an intensity of 1 mA ³⁸ using a constant-current electrical stimulator. Two 35cm² electrodes with sponge surfaces were placed over the ipsilesional supraorbital region (anodal electrode) and the contralesional (cathodal electrode) primary motor cortex using the positions of C3 or C4 electrodes of the international 10-20 EEG system ³⁹. For sham stimulation, the current was ramped up for 30 seconds and then slowly tapered down to zero. This modus operandi has been used to prevent participants from differentiating between real and sham stimulation ⁴⁰. Physical therapy was started after about 5 minutes of tDCS.

Repetitive transcranial magnetic stimulation (rTMS)

A MagPro X100 stimulator^b connected with a figure of eight coil^b (MCF-B65) or to a sham coil^b (MCF-P-B65) was used to deliver continuous theta burst stimulation (cTBS).

The cTBS protocol used in this study was the same as previously described in Nyffeler *and al.* ^{41, 42} (detailed information is listed in *Appendix I*). Each session consisted of two spaced neuronavigated^c cTBS applications, separated by 15 minutes. Paired application of cTBS has previously been shown to induce longer lasting effects as compared to a single application ^{43, 44}. For sham cTBS, the sham coil^b produced no magnetic field.

Clinical assessments

For clinical assessments, we used the following measures: Fugl-Meyer assessment of the upper extremity (UE-FMA) ⁴⁵; Box and Block Test (BBT) ⁴⁶; Nine Hole Peg Test (NHPT) ⁴⁷; Jamar dynamometer ⁴⁸. The NHPT was expressed in pegs/s. All scores were normalized to values of the unaffected arm of each subject. To obtain a multifaceted motor evaluation, each ratio was then averaged to a compound motor score (CMS).

To control for variability in spontaneous recovery, we investigated whether any of the two NIBS interventions might accelerate recovery during the treatment period as compared to the rate of improvement during baseline assessments. To this end, we computed the slope

of motor improvement as the difference between two consecutive CMS scores, divided by the time between them. The primary clinical outcome measure was defined as the difference between the slope of improvement during the treatment period and the slope during the baseline period.

Changes between pre (T2) and post intervention (T3 and T4) in each test used for computation of the CMS were used as secondary outcomes. Changes in UE-FMA were quantified as percentage of the maximum possible improvement which better reflects biological recovery processes^{49, 50}. We also acquired the Motor Activity Log-14 (MAL-14), to quantify changes in subjective real-life arm use⁵¹. Clinical effects were tested for differences between stimulation groups with an one-way ANOVA or, if data did not meet the assumption of normality, Kruskal-Wallis tests.

Electroencephalography

EEG was collected with a 128-channel Biosemi ActiveTwo EEG-system^d and sampled at 512 Hz. Participants were asked to keep their eyes closed, while remaining awake. Five-minutes of artifact-free data were recalculated against the average reference. One subject was excluded from EEG analysis because she refused to undergo post-treatment EEG recording.

Effective connectivity

Based on interhemispheric imbalance model, we estimated the influence of the contralesional primary motor cortex (M1) over the affected M1 using partial directed coherence as a multivariate measure of effective connectivity. Analyses were performed as described previously^{52, 53} and in *Appendix II*. Data from 3 out of 40 participants with available EEG had to be excluded from this analysis because of abundant high-frequency EEG artifacts. Partial directed coherence (PDC) values were log-transformed to meet the assumption of normality and subjected to parametric statistical tests to assess within group changes across time and differences between groups.

Functional connectivity

Functional connectivity (FC) was quantified as described previously^{36, 37, 54} and in *Appendix III* using the absolute imaginary component of coherence in alpha (8-12Hz) and beta bands (13–16 Hz). Interactions in these frequencies were previously found to be associated with motor behavior and recovery^{35, 36}. The graph theoretical measure of *weighted node degree* (WND) was used to quantify global FC of a brain area and computed as the sum of FC of a given voxel with all other voxels⁵⁵. Since ROI WND values were normally distributed, we used t-tests to assess within group changes across time and a one-way ANOVA to assess differences between groups. In addition, groups

were compared using voxel-wise unpaired pseudo-t-tests corrected with a cluster-based threshold for testing multiple voxels ⁵⁶.

Associations between neural and clinical effects

Relationships between the clinical variables and NIBS-induced changes in effective/functional connectivity were analyzed with Pearson's correlations. Since we recruited subjects over a period spanning several different stages of brain plasticity (2 to 10 weeks after stroke), we refined this analysis to explore the impact of the time of NIBS application. The first month after stroke provides a time window of opportunity for plastic changes ⁵⁷⁻⁵⁹. Furthermore, previous findings had suggested that beta-band coherence was associated with better motor recovery only in the first weeks after stroke, while late enhancements were even associated with worse recovery ³⁷. Subjects were therefore segregated into two groups according to the delay between stroke infarct and the first stimulation session. Correlations were then computed separately for a subgroup of patients in whom treatment could be started within the first 4 weeks after stroke and for a subgroup with later treatment onset. In addition, we computed the size of the intervention effect between NIBS groups and sham condition for the different subgroups. Statistical tests were performed using MATLAB R2012a and its statistics toolbox (Mathworks Inc, Natwick, USA).

Results

Baseline demographic, clinical, and stroke parameters were similar between groups (see Table 1). The stimulation was well tolerated. No adverse effect was observed. The lesion distribution of the subjects is depicted in the supplementary material.

Clinical effects

The baseline evaluations revealed no significant differences between the three treatment groups in the primary or any secondary outcomes measure ($N=41$, $p>0.63$) (Table 2).

Between-group analysis using Kruskal–Wallis test showed no significant difference between the three experimental groups in the primary outcome measure, the change in CMS slope ($\chi^2=0.74$, $p=0.69$) or any of the secondary outcome measures ($N=41$, $p>0.35$) (Table 3).

Effective connectivity

Prior to intervention, the pattern of endogenous effective connectivity among homologous M1 was similar for the three groups ($N=37$, $F_{2,34}=0.17$, $p=0.84$). cTBS significantly reduced

driving from contralesional M1 in the beta frequency band (mean change -1.24 ± 1.34 , 95% CI: -2.04 to -0.43 ; $t_{12}=-3.34$, $p=0.006$) while ca-tDCS significantly enhanced this influence (1.45 ± 1.97 , 95% CI: 0.26 to 2.64 ; $t_{12}=2.66$, $p=0.02$). In contrast, no significant change was observed in the sham condition (0.62 ± 2.47 , 95% CI: -1.03 to 2.28 ; $t_{10}=0.84$, $p=0.42$). There was a statistically significant difference between the groups ($F_{2,34}=6.48$, $p=0.0041$). Post hoc comparison reported that cTBS had significantly greater effect on effective connectivity between M1 cortices than ca-tDCS (95% CI: -4.05 to -1.32 ; $t_{24}=-4.07$, $p=0.0004$) and sham stimulation (95% CI: -3.5 to -0.22 ; $t_{22}=-2.35$, $p=0.03$) (Figure 2). Hence, cTBS applied to the contralesional hemisphere reduced the interaction between the stimulated site and its homologous area, as hypothesized by the model of interhemispheric imbalance after stroke. These modulations take place in beta frequencies known to be implicated in motor function^{37, 60}.

However, no association was found between the change in PDC from contralesional to ipsilesional M1 and clinical recovery, neither across all patients ($r=0.01$, $p=0.95$, uncorrected), nor across patients in the subgroups with early ($r=0.03$, $p=0.91$) or late ($r=-0.05$, $p=0.84$, uncorrected) NIBS onset. Hence, the neural effect on interhemispheric inhibition did not translate into improved motor recovery.

Functional Connectivity

Alpha and beta-band WND of the ipsilesional M1 were comparable between the 3 groups before stimulation ($N=40$, $F_{2,37}<1.1$, $p>0.35$). There was no significant change in alpha-band WND at M1 region after the intervention in any group ($p>0.31$) and there was no difference between groups ($p>0.39$). Conversely, beta-band WND tended to enhance after ca-tDCS (mean change 0.23 ± 0.46 , 95% CI: -0.04 to 0.50; $t_{13}=1.82$, $p=0.09$), while it reduced after sham stimulation (-0.25 ± 0.40 , 95% CI: -0.51 to 0.003; $t_{11}=-2.17$, $p=0.05$). No significant change was observed after cTBS (-0.17 ± 0.65 , 95% CI: -0.54 to 0.21; $t_{13}=-0.95$, $p=0.36$). There was a statistically significant difference between the groups ($F_{2,37}=3.19$, $p=0.05$). Post hoc tests revealed that the increase was significantly greater after ca-tDCS than after sham stimulation (95% CI: 0.12 to 0.83; $t_{24}=2.78$, $p=0.01$) and tended to be greater than after cTBS (95% CI: -0.05 to 0.83; $t_{26}=1.83$, $p=0.08$) (Figure 3A).

In order to explore effects in other brain areas, we also performed voxel-wise contrasts of WND changes between stimulation conditions. Figure 3B shows that NIBS also increased beta-band WND in paracentral nodes. Conversely, there was no change outside the motor networks ($p>0.05$, cluster corrected).

A Pearson correlation analysis across all patients of all groups showed that the modulation in beta-band WND was not correlated with clinical recovery ($r=-0.15$, $p=0.34$). However,

in the subgroup of patients in whom therapy was started within 4 weeks after stroke (N=15), a significant positive association between beta-band WND changes in ipsilesional M1 and the proportion of UE-FMA improvement was found ($r=0.70$, $p=0.0076$, FDR corrected). When treatment was started later, the correlation was not significant and negative (N=25, $r=-0.25$, $p=0.22$, FDR corrected). In addition, the strength of the correlation in the early subgroup was significantly greater than the correlation in the late subgroup (Fisher r -to- z transformation, $Z=-3.1$, $p<0.0017$). Furthermore, correlations were spatially specific. Beta-band WND at the supplementary motor area (SMA) ($r=0.38$, $p=0.16$, uncorrected) or inferior parietal lobule (IPL) ($r=0.12$, $p=0.68$, uncorrected) did not correlate with motor improvement for patients in the early subgroup (Figure 4A).

To further examine the impact of the delay of NIBS treatment after stroke, we assessed the clinical effect size of each active stimulation condition compared with sham stimulation as a function of the delay between stroke and treatment initiation. The effect size was large and tended to approach significance for ca-tDCS started within the first 4 weeks (Hedges' $g=1.02$, 95% CI: -0.21 to 2.22; $t_9=1.80$, $p=0.11$) and medium for cTBS started within the first 4 weeks (Hedges' $g=0.46$, 95% CI: -0.63 to 1.53; $t_{10}=0.85$, $p=0.41$). Conversely, effect sizes were close to zero or even negative when treatment was started later (ca-tDCS, Hedges' $g=-0.24$, 95% CI: -0.98 to 0.96; $t_{13}=-0.02$, $p=0.98$); cTBS, Hedges' $g=-0.01$, 95% CI: -1.21 to 0.72; $t_{14}=-0.51$, $p=0.62$) (Figure 4B).

Discussion

The present study aimed to investigate the influence of multiple sessions of ca-tDCS and cTBS over contralesional M1 on motor recovery and its underlying neural mechanisms in subacute stroke subjects. Overall, neither stimulation treatment enhanced motor gains when compared with physical therapy alone. This lack of benefit is in accordance with the inconsistency of motor improvements reported in previous trials^{14, 15, 18, 20, 61-63}. ca-tDCS and cTBS induced specific changes in neural markers of plasticity, but these neural effects did not translate into improved motor recovery at the group level. This suggests that the most commonly used neural targets of NIBS are not generally valid for a heterogeneous population of subacute stroke subjects. Yet, an exploratory subgroup analysis suggests that targeting perilesional oscillation coherence within the first 4 weeks after stroke might enable more robust effects.

Modulation of interhemispheric driving

Contrary to our initial hypothesis, only one of the two “inhibitory” protocols induced the expected decrease in interhemispheric interactions between motor nodes. This suggests that cTBS might be more efficient for decreasing influences from contralesional hemisphere as hypothesized by the interhemispheric imbalance model.

These differences between stimulation modalities are most likely due to their different modes of action ⁶⁴⁻⁶⁸. tDCS produces a weak polarization of large assemblies of neurons and modulates the on-going synaptic activity during motor activation ⁶⁹. In contrast, cTBS induces a more focal electrical field that generates action potentials in more specific neural circuits ^{64, 65}. This may be advantageous when one wants to stimulate specific white matter tracts. We may then speculate that cTBS may have more preferentially affected transcallosal neurons than ca-tDCS.

In any case, no association was found between changes in interhemispheric driving and motor improvement. These results seem in contradiction with the interhemispheric rivalry theory ²⁸⁻³⁰. However, it is important to point out that our experiment investigated the endogenous interactions between homologous brain areas. Conversely, the most influential studies revealed abnormal interaction during a pre-movement time window ³⁰. Our data may be interpreted such that abnormalities during movement do not hold true at rest. Hence, rebalancing the endogenous driving from the preserved M1 is not a direct therapeutic target towards a possible clinical improvement in subacute stroke. This conclusion is also supported by previous studies reporting an absence of interhemispheric imbalance during rest among stroke subjects in the first six months ³¹⁻³³. In addition, the interhemispheric rivalry model has been derived exclusively from chronic stroke patients with subcortical lesion and mild to moderate motor impairments. Applying the model to all patients may be an oversimplification ⁷⁰. Hence, targeting a reduction of endogenous driving from the unaffected M1 over the affected area is not systematically efficient. This

underlines the need to acquire longitudinal evidence of specific mechanisms mediating interhemispheric interaction to refine the framework.

Ipsilesional functional network plasticity

This study demonstrates that NIBS can modulate specific patterns of neural interactions. In particular, we observed significantly higher ipsilesional FC after ca-tDCS compared with the other treatments. The larger effect of ca-tDCS (applied over the contralesional M1) on perilesional networks could be due to volume conduction resulting from the relatively diffuse application setup over it could arise via interhemispheric fibers in the motor network⁷¹⁻⁷³.

Again, the modulation of perilesional coherence was not associated with improved motor recovery at the group level. Yet, previous observational studies have already demonstrated that perilesional beta-band coherence needs to be enhanced within the first weeks after stroke³⁷. Here, we reproduce this finding in an independent population and using an interventional approach, by showing that the NIBS-induced enhancement of beta-band coherence had a large effect on motor recovery only when the enhancement was achieved early. After this time window, no clinical gain compared with placebo was observed. However, these findings need to be replicated in a larger subject sample.

Taken together, these findings suggest that ca-tDCS can influence correlates of spontaneous plasticity taking place during a critical time window of opportunity for brain repair, as corroborated by microbiological studies ⁷⁴⁻⁷⁶. A potential mechanism lies in the induction of adaptive cortical plasticity which might concurrently increase functional connectivity ³⁵. Support for this hypothesis stems from animal models of stroke, which showed that tDCS can increase oligodendrocyte precursors, proliferation of endogenous neural stem cells and migration to the site of ischemic stroke *in vivo* ^{77, 78}. In contrast, if perilesional coherence is enhanced too late, it may remain inefficient because of lacking microbiological conditions for cortical repair.

Study limitations

The absence of significant clinical differences between the three groups of subjects involved in our study could be due to the small sample size. However, based on the effect sizes observed in our study, about 700 subjects would be needed in each arm in order to detect significant differences with 80% power.

We cannot extrapolate the results presented here to protocols applied to the affected hemisphere. cTBS and tDCS may show comparable effects in this case. Moreover, excitatory protocols applied to the affected hemisphere may be less time sensitive. For instance, improved clinical outcomes were observed after anodal tDCS in chronic stroke patients ^{79, 80}.

Conclusions

This study demonstrates that tDCS and rTMS can target different aspects of stroke plasticity. An inhibition of the contralesional M1 or a reduction of interhemispheric interactions did not lead to improved motor recovery in our sample. Conversely, exploratory subgroup analyses suggest that motor recovery might be enhanced by early interventions that seek to increase FC of ipsilesional motor nodes. This hypothesis will need to be confirmed in future trials applying tDCS within the first 4 weeks after stroke.

Appendix

Appendix I: Repetitive transcranial magnetic stimulation

rTMS was delivered using a theta burst stimulation (TBS) protocol. TBS is a more recent form of rTMS which has the advantage of inducing longer aftereffects while requiring shorter stimulation time than conventional rTMS^{42, 81}. When theta-burst stimulation is delivered continuously, it is expected to have a robust inhibitory effect on the underlying brain areas⁸¹. The coil was positioned over the contralesional primary motor cortex and maintained with a neuronavigation system (TMS Navigator, Localite, Bonn, Germany), based on the coregistered high-resolution 3D anatomical MRI (T1-weighted MP-RAGE). The stimulation site and the resting motor threshold were determined using a single biphasic transcranial magnetic stimulation pulse and defined as the site at which the lowest stimulus intensity produced a visible contraction of the unaffected, relaxed small hand muscles. Stimulation intensity was set to 80% of resting motor threshold. One application consisted of a continuous train of 267 bursts, each composed of three pulses applied at 30 Hz, repeated at inter-burst intervals of 167 ms. The train lasted approximately 30 seconds and consisted of 600 stimuli^{41, 42}.

Appendix II: Interhemispheric effective connectivity

Source effective connectivity was calculated in Matlab software (MathWorks, Natick, MA, USA). The lead-potential with 1 cm grid spacing was computed using 3-shell boundary element model (BEM) with the Helsinki BEM library (<http://peili.hut.fi/BEM/>)⁸² and the NUTEEG plugin of NUTMEG (<http://www.nitrc.org/plugins/mwiki/index.php/nutmeg:MainPage>), based on each subject's 3D T1-weighted MP-RAGE structural MRI. We first parcellated the brain into 84 anatomical regions and estimated the spontaneous activity at each region using an inverse solution⁸³. The solution point which was closest to the geometrical center of each region (centroid) and which was structurally intact on the coregistered MRI was considered to represent the source activity of the region. Motor regions were defined using the human motor area template⁸⁴ and the remaining non-motor areas with the Automated Anatomical Labelling template⁸⁵. In order to take the changing three-dimensional orientation of the source dipoles into account, these were projected on the predominant dipole direction of each ROI at each timepoint, to obtain scalar values of the current density^{86, 87}.

Partial directed coherence (PDC) estimates the directed functional interactions between pairs of regions that are components of a multivariate process⁸⁸. It is based on the concept of Granger-causality and computed using multivariate autoregressive (MVAR) models of an appropriate order, which simultaneously model multiple time series. The MVAR model order was defined heuristically as the minimum order that was able to

resolve not only low frequency components of the coherence spectrum but also coherence in the beta frequency range which was of particular interest for the motor system⁸⁹. We used a model of order 30, corresponding to about 60 ms of signal. This choice is in agreement with Blinowska⁹⁰: the number of data points $k \cdot N$ (k – number of regions, N – number of data points) should be at least 10 times higher than the number of parameters $k2p$ (p – model order). In our case, we had 60 times more data points than parameters. To compute the MVAR model coefficients we used the Nutall-Strand algorithm^{91, 92} and treated the 300 epochs per subject as repeated trials⁹³. We computed the squared PDC⁹⁴.

Appendix III: Ipsilesional functional connectivity

Source functional connectivity was calculated in Matlab (MathWorks, Natick, MA, USA) with the open-source toolbox NUTMEG (<http://www.nitrc.org/plugins/mwiki/index.php/nutmeg:MainPage>)⁹⁵ and its functional connectivity mapping (FCM) toolbox⁵⁴. The lead-potential with 1 cm grid spacing was computed using 3-shell boundary element model (BEM) with the Helsinki BEM library (<http://peili.hut.fi/BEM/>)⁸² and the NUTEEG plugin of NUTMEG, based on each subject's 3D T1-weighted MP-RAGE structural MRI.

EEG segments were bandpass filtered between 1 and 20 Hz and projected to source space with an adaptive spatial filter (scalar minimum variance beamformer)⁹⁶. Functional connectivity (FC) was quantified in source space using the absolute imaginary component

of coherence⁹⁷. This measure is known to avoid artificial overestimation or distortion of functional connectivity due volume conduction or spatial leakage of the inverse solution⁹⁸. From this, we computed the weighted node degree (WND) of each voxel as the sum of its coherence with all remaining cortical voxels⁵⁵. Between-participant differences in signal to noise ratio can impact functional connectivity estimates. To avoid this, we normalized maps of each patient by subtracting the mean WND across all voxels from each voxel and by dividing by the standard deviation across voxels, hence yielding z-scores. To permit group analysis, maps were spatially normalized to canonical Montreal Neurological Institute (MNI) space using functions of the toolbox SPM8 (<http://www.fil.ion.ucl.ac.uk/spm/software/spm8/>). Stroke lesions were masked during spatial normalization to avoid distortions⁹⁹. After registration to a standard space, images from patients with right hemispheric stroke were flipped about the midline in order to align all lesions to the left side of the image.

Voxel-wise FC maps was generated for each patient. In addition, ipsilesional primary motor cortex and supplementary motor area were defined as ROI with anatomical templates^{84,85}. In addition, inferior parietal lobule in the affected hemisphere was defined as nearby control ROI outside the motor network. The mean WND at each ROI was calculated as the average of its voxels.

535 References

- 536 1. Bolognini N, Pascual-Leone A, Fregni F. Using non-invasive brain stimulation to augment motor
537 training-induced plasticity. *J Neuroeng Rehabil* 2009;6:8.
- 538 2. Fregni F, Pascual-Leone A. Technology insight: noninvasive brain stimulation in neurology-
539 perspectives on the therapeutic potential of rTMS and tDCS. *Nat Clin Pract Neurol* 2007;3(7):383-93.
- 540 3. Kang N, Summers JJ, Cauraugh JH. Non-Invasive Brain Stimulation Improves Paretic Limb Force
541 Production: A Systematic Review and Meta-Analysis. *Brain Stimul* 2016;9(5):662-70.
- 542 4. Tedesco Triccas L, Burridge JH, Hughes AM, Pickering RM, Desikan M, Rothwell JC et al. Multiple
543 sessions of transcranial direct current stimulation and upper extremity rehabilitation in stroke: A
544 review and meta-analysis. *Clin Neurophysiol* 2016;127(1):946-55.
- 545 5. Wessel MJ, Zimerman M, Hummel FC. Non-invasive brain stimulation: an interventional tool for
546 enhancing behavioral training after stroke. *Front Hum Neurosci* 2015;9:265.
- 547 6. Roche N, Geiger M, Bussel B. Mechanisms underlying transcranial direct current stimulation in
548 rehabilitation. *Ann Phys Rehabil Med* 2015;58(4):214-9.
- 549 7. Liew SL, Santarnecchi E, Buch ER, Cohen LG. Non-invasive brain stimulation in neurorehabilitation:
550 local and distant effects for motor recovery. *Front Hum Neurosci* 2014;8:378.
- 551 8. Nair DG, Renga V, Lindenberg R, Zhu L, Schlaug G. Optimizing recovery potential through
552 simultaneous occupational therapy and non-invasive brain-stimulation using tDCS. *Restor Neurol*
553 *Neurosci* 2011;29(6):411-20.
- 554 9. Khedr EM, Abdel-Fadeil MR, Farghali A, Qaid M. Role of 1 and 3 Hz repetitive transcranial magnetic
555 stimulation on motor function recovery after acute ischaemic stroke. *Eur J Neurol*
556 2009;16(12):1323-30.
- 557 10. Russo C, Souza Carneiro MI, Bolognini N, Fregni F. Safety Review of Transcranial Direct Current
558 Stimulation in Stroke. *Neuromodulation* 2017.
- 559 11. Rossi S, Hallett M, Rossini PM, Pascual-Leone A. Safety, ethical considerations, and application
560 guidelines for the use of transcranial magnetic stimulation in clinical practice and research. *Clin*
561 *Neurophysiol* 2009;120(12):2008-39.
- 562 12. Oberman L, Edwards D, Eldaief M, Pascual-Leone A. Safety of theta burst transcranial magnetic
563 stimulation: a systematic review of the literature. *J Clin Neurophysiol* 2011;28(1):67-74.
- 564 13. Zimerman M, Heise KF, Hoppe J, Cohen LG, Gerloff C, Hummel FC. Modulation of training by single-
565 session transcranial direct current stimulation to the intact motor cortex enhances motor skill
566 acquisition of the paretic hand. *Stroke* 2012;43(8):2185-91.
- 567 14. Grefkes C, Nowak DA, Wang LE, Dafotakis M, Eickhoff SB, Fink GR. Modulating cortical connectivity
568 in stroke patients by rTMS assessed with fMRI and dynamic causal modeling. *Neuroimage*
569 2010;50(1):233-42.
- 570 15. Avenanti A, Coccia M, Ladavas E, Provinciali L, Ceravolo MG. Low-frequency rTMS promotes use-
571 dependent motor plasticity in chronic stroke: a randomized trial. *Neurology* 2012;78(4):256-64.
- 572 16. Fregni F, Boggio PS, Mansur CG, Wagner T, Ferreira MJ, Lima MC et al. Transcranial direct current
573 stimulation of the unaffected hemisphere in stroke patients. *Neuroreport* 2005;16(14):1551-5.
- 574 17. Takeuchi N, Tada T, Toshima M, Chuma T, Matsuo Y, Ikoma K. Inhibition of the unaffected motor
575 cortex by 1 Hz repetitive transcranial magnetic stimulation enhances motor performance and
576 training effect of the paretic hand in patients with chronic stroke. *J Rehabil Med* 2008;40(4):298-
577 303.
- 578 18. Ackerley SJ, Stinear CM, Barber PA, Byblow WD. Combining theta burst stimulation with training
579 after subcortical stroke. *Stroke* 2010;41(7):1568-72.

19. Hesse S, Waldner A, Mehrholz J, Tomelleri C, Pohl M, Werner C. Combined transcranial direct current stimulation and robot-assisted arm training in subacute stroke patients: an exploratory, randomized multicenter trial. *Neurorehabil Neural Repair* 2011;25(9):838-46.
20. Talelli P, Wallace A, Dileone M, Hoad D, Cheeran B, Oliver R et al. Theta burst stimulation in the rehabilitation of the upper limb: a semirandomized, placebo-controlled trial in chronic stroke patients. *Neurorehabil Neural Repair* 2012;26(8):976-87.
21. Hamada M, Murase N, Hasan A, Balaratnam M, Rothwell JC. The role of interneuron networks in driving human motor cortical plasticity. *Cereb Cortex* 2013;23(7):1593-605.
22. Hordacre B, Ridding MC, Goldsworthy MR. Response variability to non-invasive brain stimulation protocols. *Clin Neurophysiol* 2015;126(12):2249-50.
23. Li LM, Uehara K, Hanakawa T. The contribution of interindividual factors to variability of response in transcranial direct current stimulation studies. *Front Cell Neurosci* 2015;9:181.
24. Nicolo P, Ptak R, Guggisberg AG. Variability of behavioural responses to transcranial magnetic stimulation: Origins and predictors. *Neuropsychologia* 2015;74:137-44.
25. Rizk S, Ptak R, Nyffeler T, Schnider A, Guggisberg AG. Network mechanisms of responsiveness to continuous theta-burst stimulation. *Eur J Neurosci* 2013;38(8):3230-8.
26. Vallence AM, Goldsworthy MR, Hodyl NA, Semmler JG, Pitcher JB, Ridding MC. Inter- and intra-subject variability of motor cortex plasticity following continuous theta-burst stimulation. *Neuroscience* 2015;304:266-78.
27. Wiethoff S, Hamada M, Rothwell JC. Variability in response to transcranial direct current stimulation of the motor cortex. *Brain Stimul* 2014;7(3):468-75.
28. Duque J, Hummel F, Celnik P, Murase N, Mazzocchio R, Cohen LG. Transcallosal inhibition in chronic subcortical stroke. *Neuroimage* 2005;28(4):940-6.
29. Grefkes C, Nowak DA, Eickhoff SB, Dafotakis M, Kust J, Karbe H et al. Cortical connectivity after subcortical stroke assessed with functional magnetic resonance imaging. *Ann Neurol* 2008;63(2):236-46.
30. Murase N, Duque J, Mazzocchio R, Cohen LG. Influence of interhemispheric interactions on motor function in chronic stroke. *Ann Neurol* 2004;55(3):400-9.
31. Buetefisch CM. Role of the Contralesional Hemisphere in Post-Stroke Recovery of Upper Extremity Motor Function. *Front Neurol* 2015;6:214.
32. McDonnell MN, Stinear CM. TMS measures of motor cortex function after stroke: A meta-analysis. *Brain Stimul* 2017;10(4):721-34.
33. Stinear CM, Peto MA, Byblow WD. Primary Motor Cortex Excitability During Recovery After Stroke: Implications for Neuromodulation. *Brain Stimul* 2015;8(6):1183-90.
34. Buch ER, Liew SL, Cohen LG. Plasticity of Sensorimotor Networks: Multiple Overlapping Mechanisms. *Neuroscientist* 2016.
35. Carmichael ST, Chesselet MF. Synchronous neuronal activity is a signal for axonal sprouting after cortical lesions in the adult. *J Neurosci* 2002;22(14):6062-70.
36. Dubovik S, Pignat JM, Ptak R, Aboulafia T, Allet L, Gillibert N et al. The behavioral significance of coherent resting-state oscillations after stroke. *Neuroimage* 2012;61(1):249-57.
37. Nicolo P, Rizk S, Magnin C, Pietro MD, Schnider A, Guggisberg AG. Coherent neural oscillations predict future motor and language improvement after stroke. *Brain* 2015;138(Pt 10):3048-60.
38. Monte-Silva K, Kuo MF, Hessenthaler S, Fresnoza S, Liebetanz D, Paulus W et al. Induction of late LTP-like plasticity in the human motor cortex by repeated non-invasive brain stimulation. *Brain Stimul* 2013;6(3):424-32.
39. Nitsche MA, Liebetanz D, Lang N, Antal A, Tergau F, Paulus W. Safety criteria for transcranial direct current stimulation (tDCS) in humans. *Clin Neurophysiol* 2003;114(11):2220-2; author reply 2-3.

40. Gandiga PC, Hummel FC, Cohen LG. Transcranial DC stimulation (tDCS): a tool for double-blind sham-controlled clinical studies in brain stimulation. *Clin Neurophysiol* 2006;117(4):845-50.
41. Nyffeler T, Cazzoli D, Hess CW, Muri RM. One session of repeated parietal theta burst stimulation trains induces long-lasting improvement of visual neglect. *Stroke* 2009;40(8):2791-6.
42. Nyffeler T, Wurtz P, Luscher HR, Hess CW, Senn W, Pflugshaupt T et al. Repetitive TMS over the human oculomotor cortex: comparison of 1-Hz and theta burst stimulation. *Neurosci Lett* 2006;409(1):57-60.
43. Goldsworthy MR, Pitcher JB, Ridding MC. A comparison of two different continuous theta burst stimulation paradigms applied to the human primary motor cortex. *Clin Neurophysiol* 2012;123(11):2256-63.
44. Goldsworthy MR, Pitcher JB, Ridding MC. The application of spaced theta burst protocols induces long-lasting neuroplastic changes in the human motor cortex. *Eur J Neurosci* 2012;35(1):125-34.
45. Fugl-Meyer AR, Jaasko L, Leyman I, Olsson S, Steglind S. The post-stroke hemiplegic patient. 1. a method for evaluation of physical performance. *Scand J Rehabil Med* 1975;7(1):13-31.
46. Mathiowetz V, Volland G, Kashman N, Weber K. Adult norms for the Box and Block Test of manual dexterity. *Am J Occup Ther* 1985;39(6):386-91.
47. Oxford Grice K, Vogel KA, Le V, Mitchell A, Muniz S, Vollmer MA. Adult norms for a commercially available Nine Hole Peg Test for finger dexterity. *Am J Occup Ther* 2003;57(5):570-3.
48. Mathiowetz V, Weber K, Volland G, Kashman N. Reliability and validity of grip and pinch strength evaluations. *J Hand Surg Am* 1984;9(2):222-6.
49. Prabhakaran S, Zarahn E, Riley C, Speizer A, Chong JY, Lazar RM et al. Inter-individual variability in the capacity for motor recovery after ischemic stroke. *Neurorehabil Neural Repair* 2008;22(1):64-71.
50. Winters C, van Wegen EE, Daffertshofer A, Kwakkel G. Generalizability of the Proportional Recovery Model for the Upper Extremity After an Ischemic Stroke. *Neurorehabil Neural Repair* 2015;29(7):614-22.
51. Uswatte G, Taub E, Morris D, Vignolo M, McCulloch K. Reliability and validity of the upper-extremity Motor Activity Log-14 for measuring real-world arm use. *Stroke* 2005;36(11):2493-6.
52. Coito A, Michel CM, van Mierlo P, Vulliemoz S, Plomp G. Directed Functional Brain Connectivity Based on EEG Source Imaging: Methodology and Application to Temporal Lobe Epilepsy. *IEEE Trans Biomed Eng* 2016;63(12):2619-28.
53. Plomp G, Quairiaux C, Michel CM, Astolfi L. The physiological plausibility of time-varying Granger-causal modeling: normalization and weighting by spectral power. *Neuroimage* 2014;97:206-16.
54. Guggisberg AG, Dalal SS, Zumer JM, Wong DD, Dubovik S, Michel CM et al. Localization of cortico-peripheral coherence with electroencephalography. *Neuroimage* 2011;57(4):1348-57.
55. Newman ME. Analysis of weighted networks. *Phys Rev E Stat Nonlin Soft Matter Phys* 2004;70(5 Pt 2):056131.
56. Singh KD, Barnes GR, Hillebrand A. Group imaging of task-related changes in cortical synchronisation using nonparametric permutation testing. *Neuroimage* 2003;19(4):1589-601.
57. Biernaskie J, Chernenko G, Corbett D. Efficacy of rehabilitative experience declines with time after focal ischemic brain injury. *J Neurosci* 2004;24(5):1245-54.
58. Carmichael ST, Archibeque I, Luke L, Nolan T, Momiy J, Li S. Growth-associated gene expression after stroke: evidence for a growth-promoting region in peri-infarct cortex. *Exp Neurol* 2005;193(2):291-311.
59. Krakauer JW, Carmichael ST, Corbett D, Wittenberg GF. Getting neurorehabilitation right: what can be learned from animal models? *Neurorehabil Neural Repair* 2012;26(8):923-31.
60. Gerloff C, Bushara K, Sailer A, Wassermann EM, Chen R, Matsuoka T et al. Multimodal imaging of brain reorganization in motor areas of the contralesional hemisphere of well recovered patients after capsular stroke. *Brain* 2006;129(Pt 3):791-808.

- 675 61. Liepert J, Zittel S, Weiller C. Improvement of dexterity by single session low-frequency repetitive
676 transcranial magnetic stimulation over the contralesional motor cortex in acute stroke: a double-
677 blind placebo-controlled crossover trial. *Restor Neurol Neurosci* 2007;25(5-6):461-5.
- 678 62. Nowak DA, Grefkes C, Dafotakis M, Eickhoff S, Kust J, Karbe H et al. Effects of low-frequency
679 repetitive transcranial magnetic stimulation of the contralesional primary motor cortex on
680 movement kinematics and neural activity in subcortical stroke. *Arch Neurol* 2008;65(6):741-7.
- 681 63. Seniow J, Bilik M, Lesniak M, Waldowski K, Iwanski S, Czlonkowska A. Transcranial magnetic
682 stimulation combined with physiotherapy in rehabilitation of poststroke hemiparesis: a randomized,
683 double-blind, placebo-controlled study. *Neurorehabil Neural Repair* 2012;26(9):1072-9.
- 684 64. Di Lazzaro V, Dileone M, Pilato F, Capone F, Musumeci G, Ranieri F et al. Modulation of motor cortex
685 neuronal networks by rTMS: comparison of local and remote effects of six different protocols of
686 stimulation. *J Neurophysiol* 2011;105(5):2150-6.
- 687 65. Di Lazzaro V, Rothwell JC. Corticospinal activity evoked and modulated by non-invasive stimulation
688 of the intact human motor cortex. *J Physiol* 2014;592(19):4115-28.
- 689 66. Huerta PT, Volpe BT. Transcranial magnetic stimulation, synaptic plasticity and network oscillations.
690 *J Neuroeng Rehabil* 2009;6:7.
- 691 67. Miranda PC. Physics of effects of transcranial brain stimulation. *Handb Clin Neurol* 2013;116:353-66.
- 692 68. Terao Y, Ugawa Y. Basic mechanisms of TMS. *J Clin Neurophysiol* 2002;19(4):322-43.
- 693 69. Bikson M, Name A, Rahman A. Origins of specificity during tDCS: anatomical, activity-selective, and
694 input-bias mechanisms. *Front Hum Neurosci* 2013;7:688.
- 695 70. Di Pino G, Pellegrino G, Assenza G, Capone F, Ferreri F, Formica D et al. Modulation of brain
696 plasticity in stroke: a novel model for neurorehabilitation. *Nat Rev Neurol* 2014;10(10):597-608.
- 697 71. Caleo M. Rehabilitation and plasticity following stroke: Insights from rodent models. *Neuroscience*
698 2015;311:180-94.
- 699 72. Kim SJ, Kim BK, Ko YJ, Bang MS, Kim MH, Han TR. Functional and histologic changes after repeated
700 transcranial direct current stimulation in rat stroke model. *J Korean Med Sci* 2010;25(10):1499-505.
- 701 73. Silasi G, Murphy TH. Stroke and the connectome: how connectivity guides therapeutic intervention.
702 *Neuron* 2014;83(6):1354-68.
- 703 74. Carmichael ST. Cellular and molecular mechanisms of neural repair after stroke: making waves. *Ann*
704 *Neurol* 2006;59(5):735-42.
- 705 75. Cramer SC. Repairing the human brain after stroke: I. Mechanisms of spontaneous recovery. *Ann*
706 *Neurol* 2008;63(3):272-87.
- 707 76. Murphy TH, Corbett D. Plasticity during stroke recovery: from synapse to behaviour. *Nat Rev*
708 *Neurosci* 2009;10(12):861-72.
- 709 77. Braun R, Klein R, Walter HL, Ohren M, Freudenmacher L, Getachew K et al. Transcranial direct
710 current stimulation accelerates recovery of function, induces neurogenesis and recruits
711 oligodendrocyte precursors in a rat model of stroke. *Exp Neurol* 2016;279:127-36.
- 712 78. Rueger MA, Keuters MH, Walberer M, Braun R, Klein R, Sparing R et al. Multi-session transcranial
713 direct current stimulation (tDCS) elicits inflammatory and regenerative processes in the rat brain.
714 *PLoS One* 2012;7(8):e43776.
- 715 79. Allman C, Amadi U, Winkler AM, Wilkins L, Filippini N, Kischka U et al. Ipsilesional anodal tDCS
716 enhances the functional benefits of rehabilitation in patients after stroke. *Science translational*
717 *medicine* 2016;8(330):330re1.
- 718 80. Stagg CJ, Bachtiar V, O'Shea J, Allman C, Bosnell RA, Kischka U et al. Cortical activation changes
719 underlying stimulation-induced behavioural gains in chronic stroke. *Brain* 2012;135(Pt 1):276-84.
- 720 81. Huang YZ, Edwards MJ, Rounis E, Bhatia KP, Rothwell JC. Theta burst stimulation of the human
721 motor cortex. *Neuron* 2005;45(2):201-6.

82. Stenroos M, Mantynen V, Nenonen J. A Matlab library for solving quasi-static volume conduction problems using the boundary element method. *Comput Methods Programs Biomed* 2007;88(3):256-63.
83. Pascual-Marqui RD. Standardized low-resolution brain electromagnetic tomography (sLORETA): technical details. *Methods Find Exp Clin Pharmacol* 2002;24 Suppl D:5-12.
84. Mayka MA, Corcos DM, Leurgans SE, Vaillancourt DE. Three-dimensional locations and boundaries of motor and premotor cortices as defined by functional brain imaging: a meta-analysis. *Neuroimage* 2006;31(4):1453-74.
85. Tzourio-Mazoyer N, Landeau B, Papathanassiou D, Crivello F, Etard O, Delcroix N et al. Automated anatomical labeling of activations in SPM using a macroscopic anatomical parcellation of the MNI MRI single-subject brain. *Neuroimage* 2002;15(1):273-89.
86. Coito A, Plomp G, Genetti M, Abela E, Wiest R, Seeck M et al. Dynamic directed interictal connectivity in left and right temporal lobe epilepsy. *Epilepsia* 2015;56(2):207-17.
87. Plomp G, Leeuwen C, Ioannides AA. Functional specialization and dynamic resource allocation in visual cortex. *Hum Brain Mapp* 2010;31(1):1-13.
88. Baccala LA, Sameshima K. Partial directed coherence: a new concept in neural structure determination. *Biol Cybern* 2001;84(6):463-74.
89. McFarland DJ, Wolpaw JR. Sensorimotor rhythm-based brain-computer interface (BCI): model order selection for autoregressive spectral analysis. *J Neural Eng* 2008;5(2):155-62.
90. Blinowska KJ. Review of the methods of determination of directed connectivity from multichannel data. *Med Biol Eng Comput* 2011;49(5):521-9.
91. Marple SL, editor *Digital spectral analysis : with applications*. Englewood Cliffs: Prentice-Hall; 1987.
92. Schlogl A, Supp G. Analyzing event-related EEG data with multivariate autoregressive parameters. *Prog Brain Res* 2006;159:135-47.
93. Babiloni F, Cincotti F, Babiloni C, Carducci F, Mattia D, Astolfi L et al. Estimation of the cortical functional connectivity with the multimodal integration of high-resolution EEG and fMRI data by directed transfer function. *Neuroimage* 2005;24(1):118-31.
94. Astolfi L, Cincotti F, Mattia D, Marciani MG, Baccala LA, de Vico Fallani F et al. Assessing cortical functional connectivity by partial directed coherence: simulations and application to real data. *IEEE Trans Biomed Eng* 2006;53(9):1802-12.
95. Dalal SS, Zumer JM, Guggisberg AG, Trumpis M, Wong DD, Sekihara K et al. MEG/EEG Source Reconstruction, Statistical Evaluation, and Visualization with NUTMEG. *Comput Intell Neurosci* 2011;2011:758973.
96. Sekihara K, Nagarajan SS, Poeppel D, Marantz A. Performance of an MEG adaptive-beamformer source reconstruction technique in the presence of additive low-rank interference. *IEEE Trans Biomed Eng* 2004;51(1):90-9.
97. Nolte G, Bai O, Wheaton L, Mari Z, Vorbach S, Hallett M. Identifying true brain interaction from EEG data using the imaginary part of coherency. *Clin Neurophysiol* 2004;115(10):2292-307.
98. Sekihara K, Owen JP, Trisno S, Nagarajan SS. Removal of spurious coherence in MEG source-space coherence analysis. *IEEE Trans Biomed Eng* 2011;58(11):3121-9.
99. Brett M, Leff AP, Rorden C, Ashburner J. Spatial normalization of brain images with focal lesions using cost function masking. *Neuroimage* 2001;14(2):486-500.

765 **Suppliers list**

766

767 a. NeuroConn DC-Stimulator, GmbH, Grenzhammer 10, 98693 Ilmenau, Germany.

768 b. MagVenture A/S, Lucernemarken 15. DK-3520 Farum, Denmark.

769 c. TMS Navigator, Localite, Schloss Birlinghoven, D-53757, Sankt Augustin, Germany.

770 d. Biosemi B.V, WG-Plein 129, 1054SC, Amsterdam, Netherlands.

771 e. Mathworks Inc, Natwick, USA.

Tables

Table 1. Comparison of baseline clinical and demographic characteristics between the experimental groups (N=41). Quantitative variables are presented as mean \pm standard deviation. No significant intergroup differences were observed for baseline features ($p>0.37$).

Characteristics	cTBS	tDCS	Sham	Test used	P value
Sex (male/female)	7/7	8/6	8/5	Fisher-Freeman-Halton	p=0.85
Age (year)	62.4 \pm 12.3	68.5 \pm 10.8	64.3 \pm 17.1	ANOVA	p=0.48
Interval from stroke onset (weeks)	5.3 \pm 1.8	5.5 \pm 1.7	4.7 \pm 1.4	ANOVA	p=0.37
Side of stroke (right/left)	10/4	9/5	10/3	Fisher-Freeman-Halton	p=0.84
Infarct site (cortical/subcortical/both)	2/4/8	2/4/8	1/6/6	Fisher-Freeman-Halton	p=0.88
Infarct type (ischemic/hemorrhagic)	13/1	10/4	10/3	Fisher-Freeman-Halton	p=0.38
Dominant hand (right/left)	13/1	13/1	13/0	Fisher-Freeman-Halton	p=1
UE-FMA (baseline 1)	12.9 \pm 11.7	13.3 \pm 10.5	15.2 \pm 14.4	ANOVA	p=0.74

UE-FMA (baseline 2)	16.9 ±13.6	18.8 ±15.5	18.6 ±17.2	ANOVA	p=0.86
NIHSS on admission	12.6 ±6.2	13.5 ±6.9	12.2 ±5.1	ANOVA	p=0.85

776

777

778

779 **Table 2. Clinical outcome measures for the three stimulation groups at pre-intervention**
780 **(T2).** Non-normally variables are presented as median \pm interquartile range.

Clinical variables	Time	cTBS	tDCS	Sham	Test used	P value
CMS slope during baseline period (%)	T1 to T2	1.4 \pm 3.9	1.2 \pm 5.0	0.6 \pm 4.2	Kruskal–Wallis	p=0.75
UE-FMA ratio (%)	T2	23.5 \pm 38.0	19.0 \pm 38.0	26.0 \pm 33.5	Kruskal–Wallis	p=0.81
Jamar ratio (%)	T2	0.0 \pm 14.0	0.0 \pm 9.0	0.0 \pm 3.0	Kruskal–Wallis	p=0.63
BBT ratio (%)	T2	0.0 \pm 0.0	0.0 \pm 0.0	0.0 \pm 7.3	Kruskal–Wallis	p=0.75
NHPT ratio (%)	T2	0.0 \pm 0.0	0.0 \pm 0.0	0.0 \pm 1.3	Kruskal–Wallis	p=0.58
MAL-14 quantitative score	T2	0.2 \pm 0.4	0.3 \pm 0.7	0.0 \pm 0.6	Kruskal–Wallis	p=0.80
MAL-14 qualitative score	T2	0.2 \pm 0.4	0.2 \pm 0.4	0.0 \pm 0.5	Kruskal–Wallis	p=0.89

781 **Table 3. Change of clinical outcome measures for the three stimulation groups (N=41) at**
782 **post-intervention (T3) and follow-up (T4) as compared to the pre-intervention baseline (T2).**
783 Normally distributed values are expressed as mean \pm standard deviation. Non-normally variables
784 are displayed with median \pm interquartile range.

Clinical variables	Time	cTBS	tDCS	Sham	Test used	P value
Change in CMS slope (%/week)	T3	0.4 \pm 2.8	0.2 \pm 1.5	0.0 \pm 2.3	Kruskal–Wallis	p=0.61
UE-FMA (percentage max.)	T3	30.6 \pm 26.0	29.9 \pm 29.3	24.8 \pm 27.3	ANOVA	p=0.84
	T4	37.1 \pm 34.8	37.1 \pm 34.5	31.4 \pm 29.7	ANOVA	p=0.88
UE-FMA ratio (%)	T3	17.6 \pm 15.5	15.7 \pm 14.6	12.8 \pm 14.4	ANOVA	p=0.70
	T4	21.0 \pm 19.2	19.8 \pm 16.8	16.6 \pm 16.5	ANOVA	p=0.80
Jamar ratio (%)	T3	2.5 \pm 8.0	4.0 \pm 8.0	2.0 \pm 8.3	Kruskal–Wallis	p=0.95

	T4	7.0 ±27.0	7.5 ±15.0	3.0 ±6.8	Kruskal–Wallis	p=0.82
BBT ratio (%)	T3	6.5 ±22.0	13.0 ±30.0	0.0 ±11.5	Kruskal–Wallis	p=0.62
	T4	11.5 ±38.0	13.0 ±34.0	0.0 ±35.3	Kruskal–Wallis	p=0.74
NHPT ratio (%)	T3	0.0 ±0.0	0.0 ±9.0	0.0 ±6.8	Kruskal–Wallis	p=0.69
	T4	0.0 ±13.0	0.0 ±10.0	0 ±11.5	Kruskal–Wallis	p=0.82
MAL-14 quantitative score	T3	0.1 ±0.4	0.4 ±0.5	0.2 ±0.7	Kruskal–Wallis	p=0.35
	T4	0.6 ±1.7	0.4 ±1.0	0.8 ±1.4	Kruskal–Wallis	p=0.89
MAL-14 quantitative score	T3	0.2 ±0.7	0.3 ±0.4	0.1 ±0.6	Kruskal–Wallis	p=0.70

	T4	0.5 ±1.5	0.4 ±1.2	0.7 ±1.3	Kruskal–Wallis	p=0.94
--	-----------	----------	----------	----------	----------------	--------

785

786

Figures

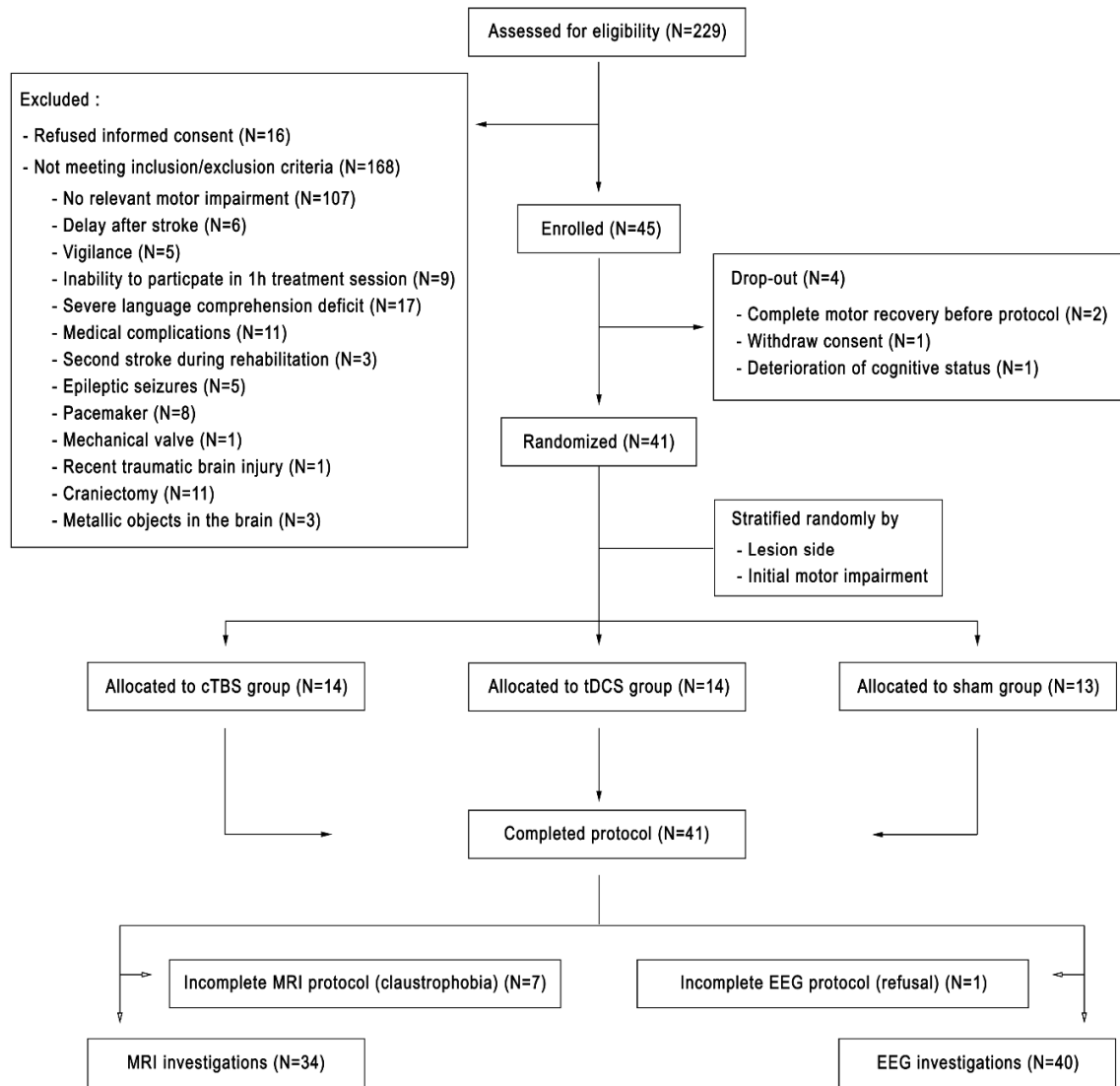


Figure 1. Patient flow through the trial.

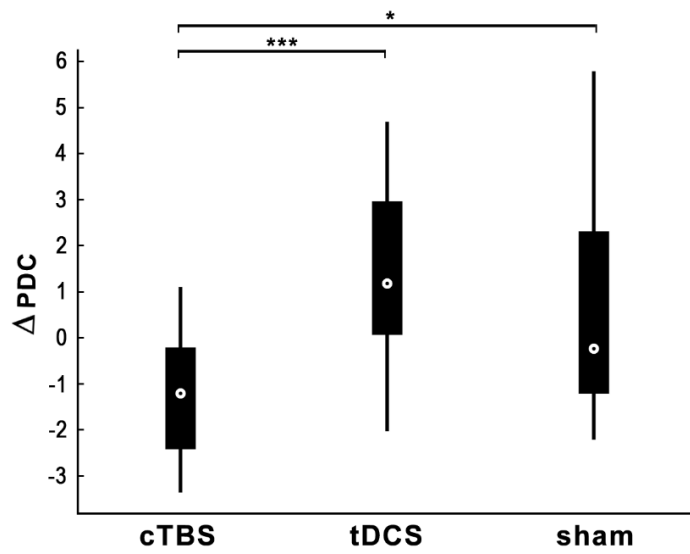
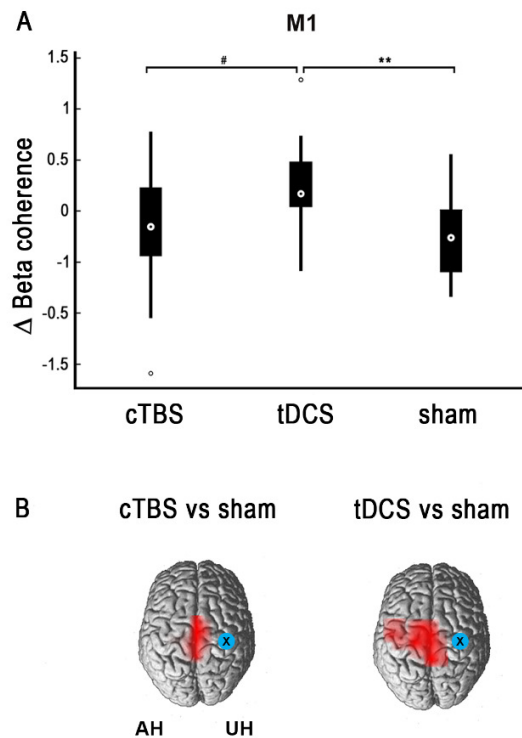


Figure 2. Changes in effective connectivity after NIBS. Patient treated with cTBS showed significantly reduced beta-band effective connectivity from contralesional primary motor cortex upon the ipsilesional primary motor area compared with ca-tDCS and sham condition (* $p < 0.05$, *** $p < 0.001$).



800

801 **Figure 3. Changes in functional connectivity after NIBS.** **A**, Patients treated with ca-
 802 tDCS showed greater enhancements of beta-band functional connectivity between the
 803 ipsilesional motor nodes and the rest of the brain compared with sham and cTBS
 804 stimulations (# $p=0.07$, ** $p<0.01$). **B**, Red color marks brain areas showing significant
 805 enhancement of beta-band functional connectivity compared to sham stimulation. All
 806 stroke lesions are aligned to the left hemisphere for visualization. The blue circle indicates
 807 the site of stimulation. *Abbreviations*: AH = affected Hemisphere, UH = unaffected
 808 Hemisphere.

809

810

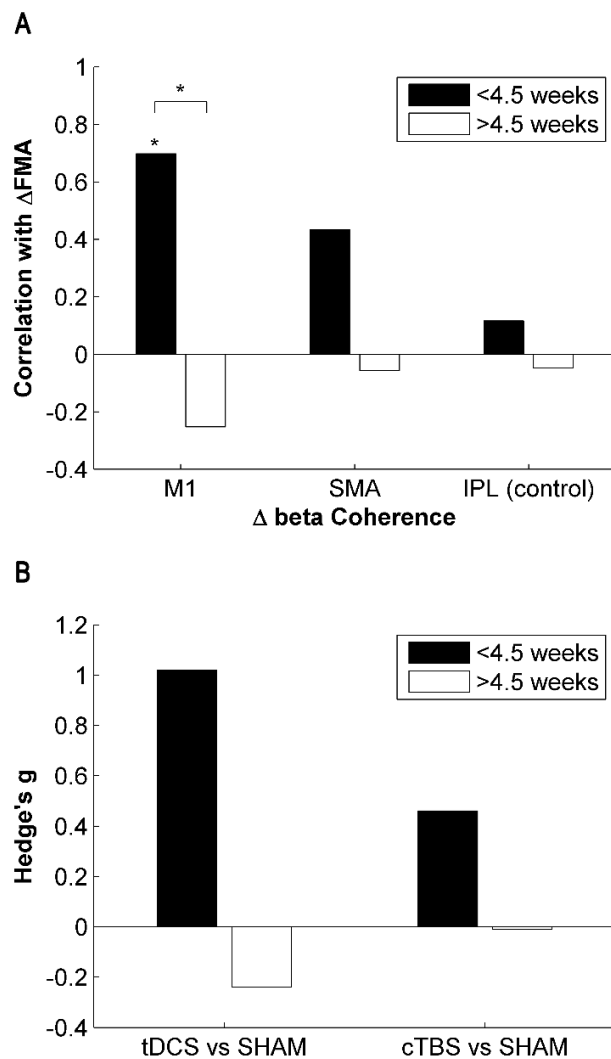


Figure 4. The importance of the time of application. **A**, Enhancements of M1 beta-band coherence were correlated with improved recovery only in patients who started NIBS within the first 4 weeks, independent of the type of treatment (* $p < 0.05$). **B**, Compared with sham stimulation, ca-tDCS had a large clinical effect size in patients who started NIBS within the first 4 weeks. This superiority disappeared at later times.